IX ECCOMAS Thematic Conference on Smart Structures and Materials
SMART 2019
A. Benjeddou, N. Mechbal and J.F. Deü (Eds)

VIBRATION SUPPRESSION AND ENERGY HARVESTING POTENTIAL IN WIND EXCITED BUILDINGS EQUIPPED WITH GROUND FLOOR TUNED INERTER DAMPER

ZIXIAO WANG[*] AND AGATHOKLIS GIARALIS[*]

[*] Department of Civil Engineering
City, University of London
Northampton Square, EC1V 0HB, London, UK
e-mail: agathoklis.giaralis.1@city.ac.uk

Key words: Tuned Inerter Damper, Optimal Vibration Control, Energy Harvesting, Weight Reduction Design, Wind Excitation, Vortex Shedding.

Abstract. This paper investigates numerically the potential of ground floor linear tuned inerter damper (TID) to mitigate floor acceleration causing occupants' discomfort in wind-excited multi-storey buildings due to vortex shedding (VS) effects while generating electric energy. To this aim, TID stiffness and damping properties were optimally designed to minimize root mean square (RMS) floor acceleration at the top occupied floor for wide range of fixed inertance values, while an electromagnetic motor (EM), modelled as an ideal damper, was added to endorse energy harvesting capabilities to the TID. Numerical data pertaining to a 15-storey steel moment resisting frame structure with square floor plan, deficient to occupants' comfort (OC) code-prescribed criteria under moderate wind action, are furnished. Wind excitation is by a spatially-correlated across-wind force field accounting for VS effects. It is found that optimally designed ground floor TID can readily meet OC criteria without any structural modification (stiffening) which for the case-study building would require 67% increase of steel weight. It is further shown that increasing EM damping coefficient increases energy harvesting potential at the expense of increased floor accelerations. However, increasing TID inertance enhances *simultaneously* floor acceleration and energy harvesting performance. Hence, it is concluded that it is possible to increase energy generation in ground floor TID-equipped wind-excited multi-storey buildings without necessarily relaxing performance requirements in terms of floor accelerations through judicial changes to EM damping coefficient and/or inertance.

1 INTRODUCTION

Design and construction of slender high-rise buildings in congested modern city centers have been gaining popularity in recent decades mostly due to ever-increasing cost of land associated with urbanization. Satisfying the structural integrity criteria under gravitational and wind design loads at the ultimate limit state is relatively straightforward in such structures using high strength materials and stiff lightweight structural components [1]. However, it is found that slender buildings with rectangular floor plan are prone to excessive oscillations in the across-wind direction (i.e., within the normal plane to the wind direction) due to vortex shedding (VS) effects generated around their corner edges [2]. These oscillations may generate floor

accelerations trespassing occupants' comfort thresholds under moderate wind action (i.e., at the serviceability limit state) [3-4] leading to loss of functionality and to downtime. Increasing the lateral stiffness of VS prone buildings cannot efficiently address serviceability performance associated with floor accelerations [5]. Therefore, dynamic vibration absorbers, with most representative the tuned mass damper (TMD), are widely used in practice for vibration mitigation in wind-excited slender buildings to meet floor accelerations thresholds prescribed by building codes and guidelines [6]. In its simplest form, the classical linear passive TMD comprises an oscillating mass attached towards the building top via linear stiffeners and viscous dampers. Stiffness and damping properties of the TMD are optimally designed/tuned to the dominant building mode shape for fixed attached mass. This provision facilitates the transfer of kinetic energy from the wind-excited building to the TMD secondary mass and, eventually, its dissipation through the dampers. Recently, the potential of TMDs to harvest energy from wind-induced oscillations in slender buildings has been explored by employing electromagnetic motors (EMs) coupled with energy harvesting/storage circuitry to replace viscous dampers in connecting the TMD mass to the host structure [7-8]. In this manner, part of the kinetic energy of the host structure is transformed into usable electric energy instead of being "lost" at the dampers in the form of heat. Moreover, Giaralis and Petrini [9-10] demonstrated that by coupling the TMD with an inerter device in the so-called tuned mass-damper-inerter (TMDI) configuration reduces significantly floor acceleration in tall/slender buildings subject to VS effects for the same attached mass. This improved vibration control efficiency of the TMDI is attributed partly to the mass-amplification effect and partly to higher-modes-damping effect endowed to the TMD by the inerter: a device developing acceleration proportional force by a coefficient termed inertance [11]. Further, Petrini et al. [12] added an EM to the TMDI and showcased significant gains in the available energy for harvesting by varying the inertance and/or the damping property of the TMDI.

Notably, all the above dynamic vibration absorbers are installed towards the top floor of buildings occupying high premium space. To address this issue, herein, the potential of a tuned inerter damper (TID), that is a TMDI with no mass property, [13] installed at the ground floor of wind-excited buildings is explored to mitigate floor accelerations at the upper floors. This consideration is inspired by several studies [13,14,15] demonstrating the high efficiency of ground floor TIDs to control earthquake-induced vibrations in multi-storey buildings. In this work, a ground floor TID is considered for the first time to control wind-induced vibrations. Furthermore, the TID is coupled with an EM to gauge its potential for harvesting energy from wind-induced oscillations. To this aim, a planar dynamical model of a 15-storey benchmark building with square floor plan deficient to floor acceleration thresholds due to VS effects is considered. Attention is focused on quantifying savings in the total weight of the structure achieved by adding a ground floor TID optimally designed for top floor acceleration reduction as opposed to increase the lateral floor stiffness. Additionally, energy harvesting potential is quantified as inertance and EM damping are let to vary.

2 BENCHMARK STRUCTURE AND WIND MODELLING

2.1 Benchmark structure description and reduced order modelling

The benchmark building considered in this paper is a doubly symmetric, 15-storey, 3-bay steel moment resisting frame (MRF) structure with 16.5m-by-16.5m footprint. It totals 49.8m

of height: ground floor is 5.0m high, while the rest of the floors are 3.2m high. The structure comprises four parallel planar MRFs along each principal axis with all beam-to-column joints taken as rigid as shown in Figure 1(a). Columns have hollow square sections with varying outer dimensions and thickness along the building height ranging between 0.48m and 0.32m, and 0.024m to 0.016m respectively. Beams are of various welded wide flange sections with section height and flange width varying between 0.5m and 0.3m, and 0.3m and 0.18m, respectively. Horizontal perfectly rigid diaphragm constraints are imposed at the height of each floor in developing a detailed finite element (FE) linear model of the structure. By deactivating the out-of-plane DOFs, the first three natural frequencies of the building and corresponding modal mass participating ratios in parentheses are 0.548Hz (0.7118), 1.391Hz (0.1675), and 2.342Hz (0.0593). The building is designed to all serviceability and ultimate limit state requirements for static design load combinations including gravitational loads and mean wind component forces acting in the along-wind direction. The required steel tonnage (MRFs self-weight) is 471tons.

To expedite computational work in later sections, a low-order planar dynamic model with 15 degrees of freedom (DOFs) corresponding to the lateral in-plane translations of the rigid slabs is derived from the detailed FE model of the benchmark building using the modal-based procedure detailed in [9]. The 15-DOF model is defined in terms of a diagonal mass matrix, and full damping matrix and stiffness matrices. Building mass including nominal gravitational loads is lumped at each floor as shown in Figure 1(b), while modal damping ratios for the j-th mode are taken as: ξ_j=1%, for j= 1,2,3; ξ_j= 2% for j= 4,5,6; ξ_j= 4% for j= 7,8,9; ξ_j=8% for j= 10,11,12; and ξ_j=16% for j= 13,14,15. The first three mode shapes obtained by the detailed FE model and the 15-DOF system match very well as shown in Figure 1(c).

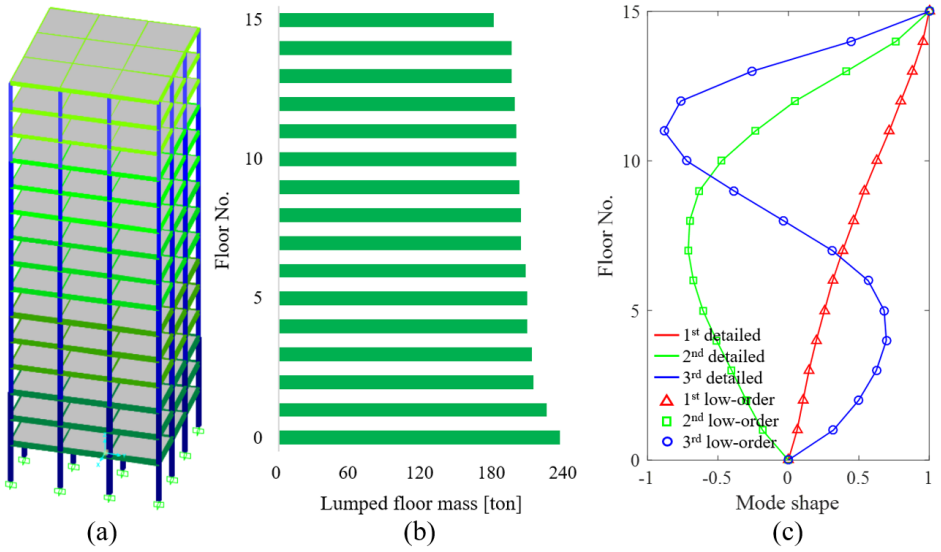

Figure 1: Benchmark building structure: (a) Detailed FE model, (b) lumped floor mass distribution along building height, (c) First three mode shapes obtained by the detailed FE and by the low-order models.

2.2 Across-wind loading model

The input wind action to the 15-storey (15-DOF) low-order model is herein represented by the stochastic across-wind force model developed in [2] for buildings with rectangular footprint.

This wind forcing model is based on experimental data from a comprehensive wind tunnel testing campaign and accounts for both the turbulence and the VS components of the wind force in the across-wind direction, the latter being critical for occupants' comfort. It is defined by a zero-mean stationary Gaussian spatially correlated random field represented in frequency domain by a full power spectral density (PSD) matrix. For the 15-DOF dynamic model, a $\mathbf{S}_{\mathbf{FF}}^{15} \in \mathbb{R}^{15\times15}$ wind force PSD matrix is determined upon spatial discretization of the wind random field at each building floor. Throughout this work, the logarithmic mean wind velocity profile of Eurocode 1 [3] is assumed for rough/urban terrain and for a (moderate) basic wind speed of 20m/s (i.e., 10mins mean wind velocity at 10m height above open flat terrain) plotted in Figure 2(a). For this wind profile, wind force PSDs at three different floor slab heights are plotted in Figure 2(b) following [2]. It is seen that the dominant VS frequency increases with floor height. The same happens for the wind force amplitude except from the last floor whose tributary height is only 1.6m. That is, half of the tributary height of typical floors.

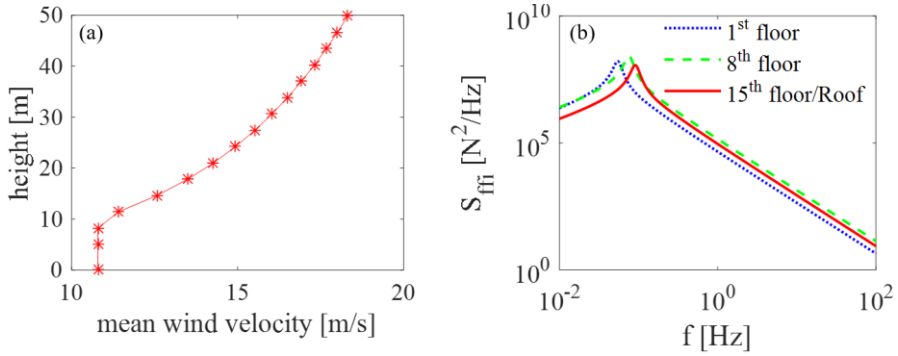

Figure 2: Assumed wind excitation model: (a) mean wind velocity profile, (b) power spectral density functions (PSDs) of across-wind forces acting at different floor levels of the benchmark structure.

2.3 Optimal re-design of benchmark structure for occupants' comfort

Whilst the case-study building in Figure 1 satisfies all requirements for *static* design load combinations, it is found to be deficient for the occupants' comfort serviceability limit state for the wind action defined in Figure 2 according to the ISO Standard 6897 [3] criteria. Figure 3(a) reports the root mean square (RMS) accelerations developing at each floor of the structure (initial structure) along its height together with the ISO 6897 occupants' comfort threshold: it is seen that RMS acceleration is over the threshold at the top two floors.

To this end, the structure is herein re-designed to satisfy the ISO6897 occupants' comfort criteria. This is achieved by using the optimal design method in [16] for MRFs with fixed layout which is based on the optimality criteria (OC) formulation in [17]. The method seeks to minimize the total structural weight while satisfying design constraints including RMS floor acceleration being below the ISO6897 threshold at all floors below the top one (roof) which is not occupied. Figure 3(b) shows the MRF self-weight variation (steel tonnage of lateral load resisting system) throughout the iterations of the optimization starting with the initial deficient design with total weight of 471tons and fundamental frequency 0.548 Hz. The iterative optimization process converges at 786tons of MRF self-weight with fundamental frequency increased to 0.920Hz after 20 design cycles. Consideration of further cycles does not improve much the self-weight. Figure 3(a) plots RMS floor accelerations of the final optimally designed

structure along with the corresponding ISO6897 threshold. The latter has increased since the re-designed structure is stiffer. It is confirmed that in the re-designed structure code-prescribed threshold for RMS floor acceleration is satisfied in all occupied floors, while floor accelerations reduce noticeably compared to the initial structure. However, this is achieved at the expense of using an additional 315tons of steel (i.e., 67% increase of steel tonnage). In following sections, an optimally designed ground floor TID is considered to meet occupants' comfort requirements without demanding additional material to stiffen the MRF load-resisting system of the initial structure without any stiffening of the MRF load-resisting system of the initial structure.

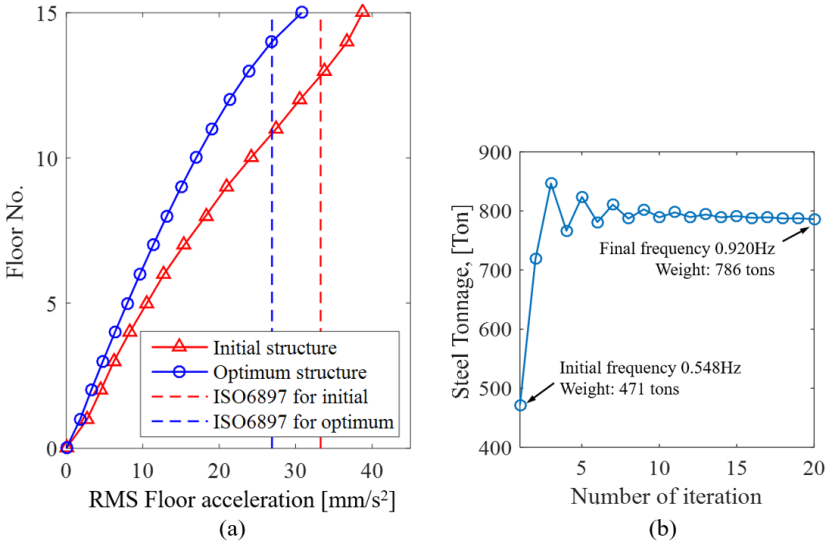

Figure 3: (a) root mean square floor accelerations of initial and optimally re-designed structures with occupants' comfort thresholds (b) Variation of total weight of structure throughout the optimal re-design process.

3 TID-EQUIPPED STRUCTURE AND FREQUENCY-DOMAIN ACROSS-WIND RESPONSE ANALYSIS

The tuned inerter damper (TID) is a linear passive dynamic vibration absorber introduced in [13] for suppressing the lateral motion of seismically excited multi-storey buildings. Herein, a TID installed at the ground floor of the ISO6897 deficient structure in Figure 1 is considered to mitigate wind-induced accelerations in the across-wind direction. TID modelling and its incorporation to the adopted structure is graphically shown in Figure 4(a) depicting the low-order 15-DOF model discussed in section 2.1 as a planar 15-storey frame-like building with lumped floor masses m_k, k=1,2,…,15, and lateral floor displacements x_k. The TID consists of a visco-elastic link, modelled as a linear spring with k_{TID} stiffness in parallel with a dashpot with damping coefficient c_{TID}, which connects one terminal of an inerter device, highlighted in red in Figure 4(a), with the first building slab. The second inerter terminal is fixed to the ground. The inerter device is idealized by a mechanical element resisting relative acceleration at its two ends through the inertance coefficient b [11]. In this regard, the inerter element force reads as

$$F_b = b\ddot{x}_{TID} \tag{1}$$

where x_{TID} is the lateral TID displacement shown in Figure 4(a) and a dot over a symbol signifies differentiation with respect to time. Therefore, the (control) inerter force depends on the inertance which may be interpreted as a "weightless mass" [11].

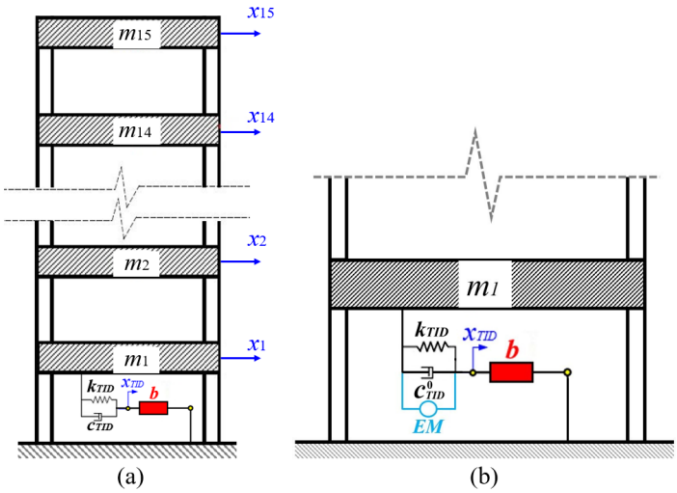

Figure 4: (a) Ground floor TID-equipped lumped-mass planar frame model of the wind-excited case-study building in the across-wind direction, and (b) Considered energy harvesting enabled TID with EM.

In this regard, it is important to note that inertance is readily scalable. Indeed, supplemental damping devices for seismic protection of building structures incorporating inerters with several hundred thousand tons of inertance have been prototyped and experimentally verified in recent years [18]. To shed further light on this issue, consider a commonly used inerter device embodiment employing a rack-and-pinion mechanism to transform the translational motion into rotational motion of a flywheel (i.e., a solid spinning disk) through a gearbox [11]. It can be readily shown that the inertance of such device is given as [19]

$$b = m_f \frac{\gamma_f^2}{\gamma_{pr}^2} \left(\prod_{q=1}^{n} \frac{r_q^2}{pr_q^2}\right), \tag{2}$$

where m_f and γ_f are the mass and radius of the gyration of the flywheel, respectively, γ_{pr} is the radius of gyration of the flywheel pinion, $r_q/(pr_q)$ is the gearing ratio of the q-th stage/gear of the gearbox with n stages. Clearly, the inertance can be scaled by orders of magnitude through changing the gearing ratios and/or the number of gears. Along these lines, Brzeski et al. [20] demonstrated experimentally the feasibility of inerter devices with continuously varying transmission gearbox, rather than stepped gearing changes, leading to inerters that may achieve any desired inertance value within the gearbox effective range of transmission.

Mathematically, the mass, **M**, damping, **C**, and stiffness, **K**, matrices of the TID-equipped lumped-mass 15-DOF model in Figure 4(a) are given as

$$\mathbf{M}=\begin{bmatrix} b & 0 & 0 & \cdots & 0 & 0 \\ & m_1 & 0 & \cdots & 0 & 0 \\ & & m_2 & \cdots & 0 & 0 \\ & & & \ddots & \vdots & \vdots \\ & SYM & & & m_{14} & 0 \\ & & & & & m_{15} \end{bmatrix},\ \mathbf{C}=\begin{bmatrix} c_{\mathrm{TID}} & -c_{\mathrm{TID}} & \cdots & \cdots & 0 & 0 \\ & c_{1,1}+c_{\mathrm{TID}} & c_{1,2} & \cdots & c_{1,14} & c_{1,15} \\ & & c_{2,2} & \cdots & c_{2,14} & c_{2,15} \\ & & & \ddots & \vdots & \vdots \\ & SYM & & & c_{14,14} & c_{14,15} \\ & & & & & c_{15,15} \end{bmatrix},$$
$$\text{and } \mathbf{K}=\begin{bmatrix} k_{\mathrm{TID}} & -k_{\mathrm{TID}} & \cdots & \cdots & 0 & 0 \\ & k_{1,1}+k_{\mathrm{TID}} & k_{1,2} & \cdots & k_{1,14} & k_{1,15} \\ & & k_{2,2} & \cdots & k_{2,14} & k_{2,15} \\ & & & \ddots & \vdots & \vdots \\ & SYM & & & k_{14,14} & k_{14,15} \\ & & & & & k_{15,15} \end{bmatrix} \tag{3}$$

respectively, where $c_{k,p}$ and $k_{k,p}$ with k=1,…,15 and p=1,…,15 are the damping and stiffness coefficients of the low-order 15DOF system representing the benchmark building. Response displacement, velocity, and acceleration PSD matrices of the TID-equipped structure subject to the wind force PSD matrix defined in section 2.2 can be obtained as

$$\mathbf{S}_{\mathbf{xx}}(\omega)=\mathbf{B}(\omega)^{*}\,\mathbf{S}_{\mathbf{FF}}(\omega)\mathbf{B}(\omega),\quad \mathbf{S}_{\dot{\mathbf{x}}\dot{\mathbf{x}}}(\omega)=\omega^2\mathbf{S}_{\mathbf{xx}}(\omega),\quad \text{and}\quad \mathbf{S}_{\ddot{\mathbf{x}}\ddot{\mathbf{x}}}(\omega)=\omega^4\mathbf{S}_{\mathbf{xx}}(\omega) \tag{4}$$

respectively. In Eq. (4), $\mathbf{S_{FF}}$ is the wind force PSD matrix $\mathbf{S}_{\mathbf{FF}}^{15}$ augmented by an upper zero row and a left-most zero column corresponding to the x_{TID} displacement DOF as the TID is internally housed and not subjected to any wind load. Further, the "*" superscript denotes complex matrix conjugation, and the transfer matrix $\mathbf{B}$ is given as

$$\mathbf{B}(\omega)=\left[\mathbf{K}-\omega^2\mathbf{M}+i\omega\mathbf{C}\right]^{-1} \tag{5}$$

where, $i=\sqrt{-1}$, and the "-1" superscript denotes matrix inversion. The RMS response velocity, and acceleration of the k-th DOF for the TID-equipped structure are obtained as

$$\mathrm{RMS}\{\dot{x}_k\}=\sigma_{\dot{x}_k}=\sqrt{\int_0^{\omega_{\max}} S_{\dot{x}_k\dot{x}_k}(\omega)\,d\omega}\quad\text{and}\quad \mathrm{RMS}\{\ddot{x}_k\}=\sigma_{\ddot{x}_k}=\sqrt{\int_0^{\omega_{\max}} S_{\ddot{x}_k\ddot{x}_k}(\omega)\,d\omega} \tag{6}$$

respectively. That is, by integrating the response auto-spectra in the main diagonal of the response velocity and acceleration PSD matrices in Eq. (4) to a cut-off frequency, ω_{max}, above which the energy of the underlying processes is negligible. Further, the relative RMS velocity between two different DOFs k and j is obtained as

$$\mathrm{RMS}\{\dot{x}_k-\dot{x}_q\}=\sigma_{\dot{x}_{kq}}=\sqrt{\sigma_{\dot{x}_k}^2+\sigma_{\dot{x}_q}^2-2\int_0^{\omega_{\max}} S_{\dot{x}_k\dot{x}_q}(\omega)\,d\omega} \tag{7}$$

where the integrand is the response velocity cross-spectra between k and q DOFs.

4 OPTIMAL TID DESIGN FOR VIBRATION CONTROL

In this section, the properties of the ground floor TID in Figure 4(a) are optimally designed to mitigate floor accelerations in multi-storey buildings subject to VS effects associated with

occupants' comfort. To this aim, an optimal design problem is formulated aiming to minimize the RMS floor acceleration of the highest occupied floor taken as the objective function (OF). This is because RMS acceleration increases monotonically with building height in the across-wind direction of typical multi-storey buildings prone to VS effects (see e.g. Figure 3(a)). The problem design variables (DVs) are the non-dimensional TID parameters defined as

$$\beta = \frac{b}{M_{tot}}, \quad \nu_{\mathrm{TID}} = \frac{\sqrt{k_{\mathrm{TID}}/b}}{\omega_1}, \quad \text{and } \xi_{\mathrm{TID}} = \frac{c_{\mathrm{TID}}}{2\sqrt{k_{\mathrm{TID}}b}}, \tag{6}$$

namely, inertance ratio, frequency ratio, and damping ratio, respectively. In the last equation, M_{tot} is the total mass of the building (including design dead and live loads), while ω_1 is the first natural frequency of the uncontrolled (no TID-equipped) structure. The optimization problem is solved numerically using the pattern search algorithm [21] to determine optimal primary DVs frequency ratio, ν_{TID}, and damping ratio, ξ_{TID}, which minimize the OF for fixed building structure, wind excitation, and inertance ratio β treated as secondary DV.

To exemplification of the above TID optimal design problem, Figure 5 furnishes results from application to the 15-storey structure discussed in section 2.1 under the wind force PSD matrix in section 2.2 to minimize $\mathrm{RMS}\{\ddot{x}_{14}\}$ computed by Eq.(6). In doing so, practically meaningful range of values for the primary DVs are searched: ν_{TID} is bounded in the [0.9, 1.1] range based on real-life TMD installations in high-rise buildings tuned to the first natural frequency ω_1, while ξ_{TID} is bounded in the [0.0, 0.2] range to ensure realistic viscous damping coefficients. Strong convex behavior of the OF on the primary DVs, ν_{TID}-ξ_{TID}, plane is noted with a single global optimal design point readily identified for inertance ratios β ranging within [0,1] interval. For illustration, $\mathrm{RMS}\{\ddot{x}_{14}\}$ surface of the TID-equipped structure normalized by $\mathrm{RMS}\{\ddot{x}_{14}\}$ of the uncontrolled structure is plotted in Figure 5(a) on the ν_{TID}-ξ_{TID} plane for β=0.2. Further, optimal DV values are plotted in Figure 5(b) as functions of β.

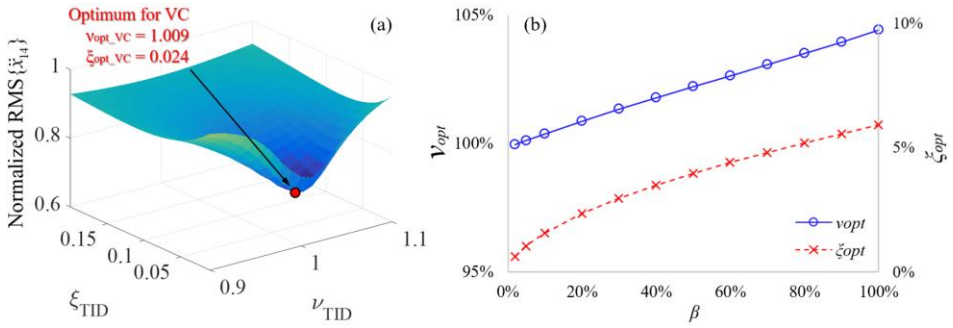

Figure 5: Optimal TID design for structure in Figure 1 subject to wind excitation in Figure 2: (a) Objective function and optimal design point for β=0.20, and (b) optimal primary DV values with β.

5 PERFORMANCE ASSESSMENT OF OPTIMAL TID-EQUIPPED BENCHMARK STRUCTURE

5.1 Vibration suppression efficiency of ground-floor TID

In this section, the potential of ground-floor TID to satisfy occupants' comfort criteria with no further structural modification in wind-excited multi-storey buildings sensitive to VS effects

is numerically assessed. Attention is focused on demonstrating that ground floor TID can support lightweight slender building designs compliant to occupants' comfort serviceability criteria leading to reduced steel usage. To this aim, optimally designed TIDs obtained as detailed in the previous section are considered for the 15-storey structure of Figure 1 which was found to be deficient to the ISO6897 occupants' comfort criteria, as seen in Figure 3(a), for the moderate across-wind excitation in Figure 2.

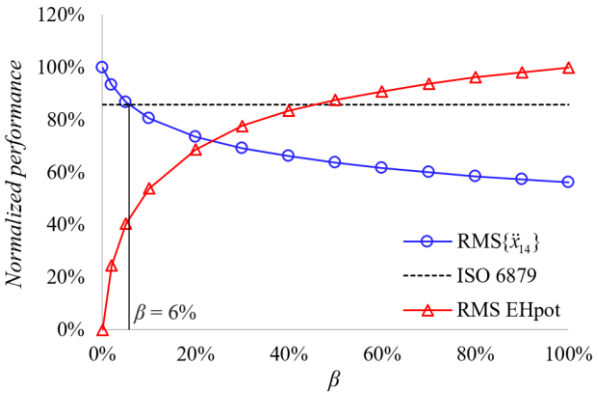

Figure 6: Normalized RMS floor acceleration at penultimate floor and available RMS energy for harvesting for TID-equipped structure in Figure 1 subject to wind forcing of Figure 2.

Figure 6 plots RMS acceleration at the penultimate (last occupied) floor of the optimal TID-controlled structure, $\mathrm{RMS}\{\dot{x}_{14}\}$, normalized by the corresponding value of the uncontrolled structure, as a function of inertance ratio. In this graph, the limiting case of $\beta = 0$ corresponds to the uncontrolled structure. It is seen that floor acceleration reduces monotonically with the inertance though performance improvement saturates as inertance ratio increases. Notably the inertance values examined in Figure 6 are realistic: even the case of β= 100%, which reduces floor acceleration by 44.8% compared to the uncontrolled structure, is achievable. Indeed, this inertance ratio corresponds to inertance $b=M_{tot}$=3285tons which is below the inertance achieved by the hydraulic inerter device discussed in [18]. However, a reduction of 14.2% in 14th floor RMS acceleration is required for the considered benchmark structure to meet ISO6879 occupants' comfort criteria. This is achieved by equipping the initial structure with an optimally tuned TID with β= 6% (or b=197tons), as indicated in Figure 6, without altering in any other way the MRF lateral load-bearing system. Recalling that meeting ISO6879 criteria through structural modification would require 315tons of additional steel to stiffen the initial MRF if no TID is installed, as discussed in section 2.3, one concludes that optimal ground-floor TID is quite efficient in meeting occupants' comfort criteria in wind excited buildings leading to lightweight designs and material savings.

5.2 Energy harvesting potential for TID with varying inertance and damping coefficient

Having established the benefits of the TID for suppressing floor accelerations in wind-excited tall buildings, the attention is now turned to explore its potential for harvesting energy from wind-borne building oscillations. To this aim, a standard linear translational EM coupled with an energy harvesting (EH) circuit is added in parallel to the visco-elastic TID element as

shown in Figure 4(b). The considered EM consists of a moving magnet travelling within a coil while the EH circuit is equipped with a rectifier to ensure unidirectional electric current flow irrespective of the magnet direction of motion [22]. The resistance of the EM is equal to R_C while EM inductance is negligible for the motion frequencies in the application at hand [22]. Moreover, the EH circuit is assumed to be purely resistive with resistance R_L: a simplification deemed sufficient for the comparative quantification of the available energy for harvesting as TID properties are let to vary (see also [8]). Under the above assumptions, the electromechanical damping coefficient of the EM coupled with the EH circuit is given as [22]

$$c_{EM} = \frac{J^2}{(R_C + R_L)} \tag{8}$$

where J is the magnetic field in the EM with constant flux density, and the resisting damping force contributed by the EM element to the structure in Figure 4 reads as

$$F_{EM} = c_{EM}(\dot{x}_1 - \dot{x}_{TID}) \tag{9}$$

Then, structural analysis to wind excitation remains the same as in section 3 by setting

$$c_{TID} = c_{TID}^0 + c_{EM} \tag{10}$$

where c_{TID}^0 is the TID viscous damping coefficient, as shown in Figure 4(b) and the RMS value of the available energy for harvesting, EHpot, is quantified as

$$\text{RMS}\{\text{EHpot}\} = c_{EM}\left(\text{RMS}\{\dot{x}_1 - \dot{x}_{TID}\}\right)^2 \tag{11}$$

making use of Eq.(7).

Figure 6 plots the RMS of EHpot for optimal TID-controlled case-study building against the inertance ratio normalized by the value attained for β=1. In obtaining this data, it is assumed that the EM contributes to half of the (optimal) TID damping, that is, $c_{TID}^0 = c_{EM}$ in Eq.(10), following optimal EH criteria [22]. It is seen that EHpot increases monotonically with inertance and, therefore, increasing inertance is beneficial for both vibration suppression and for energy harvesting in ground floor TID optimally designed for vibration suppression.

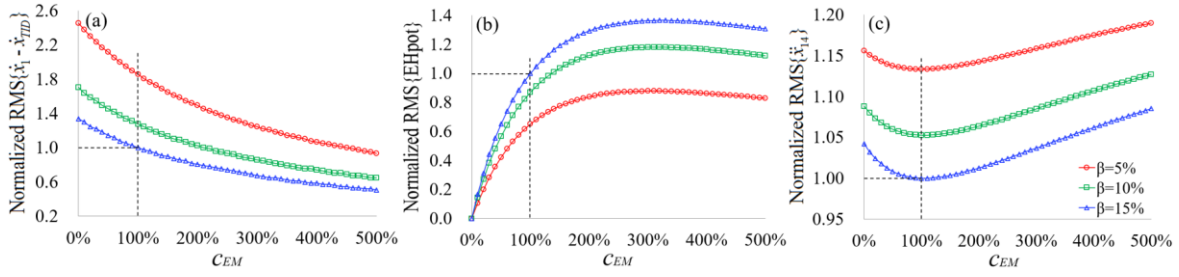

Figure 7: Normalized EH potential and performances of the EH-TID for v_b = 20m/s, β=0.05, 0.10, and 0.15, and for (a) RMS relative velocity, (b) RMS EH potential, and (c) RMS acceleration at the last occupiable floor.

Moreover, Figure 7 quantifies RMS EHpot and penultimate RMS floor acceleration for non-optimal TID-equipped structure as c_{EM} in Eq.(9) is let to vary for fixed k_{TID} and c_{TID}^0, and for three different β values. Values of k_{TID} and c_{TID}^0 are optimal for TID with β=15% and all plotted quantities are normalized to the attained values for this optimal TID design including the value

of c_{EM}. This investigation is motivated by the fact that both the c_{EM} in Eq.(9) and the inertance b in Eq.(2) can vary in a passive-adaptive mode by changes to the EH circuit and to the inerter gearing, respectively. It is seen in Figure 7(b) that ncreases with c_{EM} until it reaches a plateau due to reduction of $\text{RMS}\{\dot{x}_1 - \dot{x}_2\}^2$ with c_{EM} in Figure 7(a). At the same time, as expected, RMS floor acceleration in Figure 7(c) increases as c_{EM} deviates from its optimal value. Nevertheless, for a fixed, possibly non-optimal, c_{EM}, *simultaneously* enhanced vibration suppression performance and increased *EHpot* is achieved by increasing inertance. These observations suggest that it is possible to increase energy generation in ground floor TID-equipped wind-excited multi-storey buildings without necessarily relaxing performance requirements in terms of floor accelerations through judicial changes to EM damping coefficient and/or inertance.

6 CONCLUDING REMARKS

The efficacy of a ground floor TID to achieve occupants' comfort performance and to harvest kinetic energy in wind-excited multi-storey buildings susceptible to VS effects has been numerically established. To this aim, a 15-storey steel structure, deficient to occupants' comfort code-prescribed criteria for moderate wind action, has been equipped with optimal TID stiffness and damping properties minimizing floor acceleration in the across-wind direction, being critical for occupants' comfort, for fixed inertance. Further, the TID was coupled with a standard EM modelled as a damper and allowing for energy harvesting. Major conclusions in view of the herein furnished numerical results are: (1) Optimally tuned TID for floor acceleration minimization is a potent retrofitting measure to meet occupants' comfort criteria without structural modifications leading to considerable increase of steel usage (up to 67% increase for the considered structure), (2) Increasing TID inertance is beneficial for both suppressing floor accelerations and for increasing available energy for harvesting in both optimal and non-optimal TID for floor acceleration mitigation, and (3) Increasing the EM damping coefficient increases the available energy for harvesting at the expense of increased floor accelerations. Overall, it is concluded that ground floor TID is a promising dynamic vibration absorber configuration for occupants' comfort criteria which govern the design of slender multi-storey buildings with square floor plan under wind excitation while allows for generating energy from wind-induced building oscillations. Still, further numerical and experimental work is warranted to examine ground-floor TID efficiency for different wind excitation intensity in a performance-based design context and to compare it to alternative widely used solutions such as top-floor TMDs.

REFERENCES

[1] Taranath, B.S. *Tall Building Design: Steel, Concrete, and Composite Systems.* CRC Press, (2017).

[2] Liang, S., Liu, S., Li, Q-S., Zhang, L., and Gu, M. *Mathematical model of across-wind dynamic loads on rectangular tall buildings. J. Wind Eng. Ind. Aerodyn.* (2002) **90**: 201-251.

[3] CEN, Eurocode 1: Action on Structures – Part 1-4: General actions – Wind actions. EN 1991-1-4:2005, Comit.

[4] ISO, Guidelines for the evaluation of the response of occupants of fixed structures to low frequency horizontal motion (0.063 to 1 Hz). ISO Standard 6897 1984, International

Organization of Standardization.
[5] Ricciardelli, F., Pizzimenti, A.D., and Mattei, M. *Passive and active mass damper control of the response of tall buildings to wind gustiness. Eng. Struct.* (2003) **25**: 1199–1209.
[6] Huang, M-F. *High-rise buildings under multi-hazard environment.* Springer Nature, (2017).
[7] Tang, X. and Zuo, L. *Simultaneous energy harvesting and vibration control of structures with tuned mass dampers. J. Intell. Mater. Syst. Struct.* (2012) **23(18)**: 2117–2127.
[8] Shen, W., Zhu, S., Xu, Y-L., and Zhu, H-P. *Energy regenerative tuned mass dampers in high-rise buildings. Struct. Control Hlth. Monit.* (2018) **25(1)**: e2072.
[9] Giaralis, A. and Petrini, F. *Wind-induced vibration mitigation in tall buildings using the tuned mass-damper-inerter (TMDI). J. Struct. Eng. ASCE* (2017) **143(9)**: 04017127.
[10] Giaralis, A. and Petrini, F. *Optimum design of the tuned mass-damper-inerter for serviceability limit state performance in wind-excited tall buildings. Procedia Engineering* (2017) **199**: 1773-1778.
[11] Smith, M.C. *Synthesis of mechanical networks: The Inerter. IEEE Transactions on Automatic Control* (2002) **47**: 1648-1662.
[12] Petrini, F., Wang, Z-X., and Giaralis, A. *Simultaneous vibration suppression and energy harvesting in wind excited tall buildings equipped with the tuned mass damper inerter (TMDI). Proceedings of the 15th Conference of the Italian Association for Wind Engineering- INVENTO*. Springer International Publishing, (2018).
[13] Lazar, I.F., Neild, S.A., and Wagg D.J. *Using an inerter-based device for structural vibration suppression. Earthquake Eng. Struct. Dyn.* (2014) **43(8)**: 1129-1147.
[14] Zhang, S-Y., Jiang, J-Z., and Neild, S. *Optimal configurations for a linear vibration suppression device in a multi-storey building. Struct. Control Hlth. Monit.* (2017) **24(3)**: 1545-2255.
[15] Giaralis, A. and Taflanidis, A. *Optimal tuned mass-damper-inerter (TMDI) design for seismically excited MDOF structures with model uncertainties based on reliability criteria. Struct. Control Hlth. Monit.* (2018) **25(2)**: e2082.
[16] Chan, C-M. and Chui, J-K-L. *Wind-induced response and serviceability design optimization of tall steel buildings. Eng. Struct.* (2006) **28**: 503-513.
[17] Venkayya, V.B. *Optimality Criteria: a basic multidisciplinary design optimization. Comput. Mech.* (1989) **5**: 1-21.
[18] Nakaminami, S., Kida H., Ikago K., and Inoue N. *Dynamic Testing of a Full-scale Hydraulic Inerter-Damper for the Seismic Protection of Civil Structures. 7th International Conference on Advances in Experimental Structural Engineering* (2017).
[19] Marian, L. and Giaralis, A. *The tuned mass-damper-inerter for harmonic vibrations suppression, attached mass reduction, and energy harvesting. Smart Structures and Systems* (2017) **19(6)**: 665-678.
[20] Brzeski, P., Lazarek, M., and Perlikowski, P. *Experimental study of the novel tuned mass damper with inerter which enables changes of inertance, J. Sound Vib.*(2017) **404**: 47–57.
[21] Charles, A. and Dennis Jr., J.E. *Analysis of Generalized Pattern Searches. SIAM Journal on Optimization.* (2003) **13(3)**: 889–903.
[22] Gonzalez-Buelga, A., Clare, L.R., Cammarano, A., Neild, S.A., Burrow, S.G., and Inman, D.J. *An optimised tuned mass damper/harvester device. Struct. Control Hlth. Monit.* (2014) **21(8)**:1154-1169.